LIQUID CRYSTALS, 2003, VOL. 30, NO. 1, 39–48

Taylor & Francis
Taylor & Francis Group

A comparison of mesogenic properties for one- and two-ring dipentyl derivatives of *p*-carboranes, bicyclo[2.2.2]octane, and benzene

WIKTOR PIECEK§, JACOB M. KAUFMAN and PIOTR KASZYNSKI*

Organic Materials Research Group, Department of Chemistry,
Vanderbilt University, Box 1822 Station B, Nashville, TN 37235, USA

A series of nonpolar single- and two-ring dipentyl derivatives of *p*-carboranes, bicyclo[2.2.2]-octane and benzene was investigated in the pure state and in binary mixtures with a nematic host. The resulting virtual nematic-isotropic transition temperatures [T_{NI}] for single ring compounds were compared with those for two ring compounds. All [T_{NI}] were compared with the molecular aspect ratios X and filling fractions F obtained from MNDO calculations. The highest effectiveness in promotion of the nematic phase was found for bicyclo[2.2.2]octane and 12-vertex *p*-carborane and ascribed to exceptional molecular rigidity and electronic properties, respectively. Results show that a high filling fraction F and molecular stiffness are the necessary factors for a highly stable nematic phase.

1. Introduction

During the past several years we have demonstrated that *p*-carboranes **1**[**1**]**a** and **2**[**1**]**a** used as structural elements promote the formation of liquid crystalline phases [1]. Available data for pure isostructural compounds suggest that the effectiveness of *p*-carboranes in stabilization of mesophases is generally lower that of bicyclo[2.2.2]octane (BCO, **3**[**1**]**a**). Moreover, 12-vertex carborane **1**[**1**]**a** typically performs better than the 10-vertex analog **2**[**1**]**a**, which is in contrast with expectations based on molecular dimensions of the clusters [2]. To gain a better understanding of the role of the carborane rings in mesophase stabilization, we have studied a series of simple one- or two-rings non-polar compounds (figure 1) in which the number of molecular variables is reduced to a minimum [2, 3].

Our earlier studies led to the conclusion that the observed ability to stabilize a nematic phase (BCO > 12-vertex > 10-vertex > Ph) can be attributed to differences in conformational and quadrupolar properties of the rings. Experimental and computational analysis shows that both of these properties appear to be more favorable in the 12-vertex than in the 10-vertex carborane, while alkyl derivatives of bicyclo[2.2.2]octane are the most conformationally rigid [4].

In another approach to compare the structural units, we studied the effect of addition of a ring to the molecule on mesophase stability [3]. Since some materials were not available, the correlation had a number of assumptions. Firstly, the comparison was done for [**1**]**b** and [**2**]**c** derivatives, secondly, there was no distinction made between the smectic and nematic phases and only clearing transitions were considered. The conclusion was that BCO stands out in the series due to changes in the distribution of conformational minima. To provide a more consistent and reliable comparison between the homologous series of compounds and to study the structural

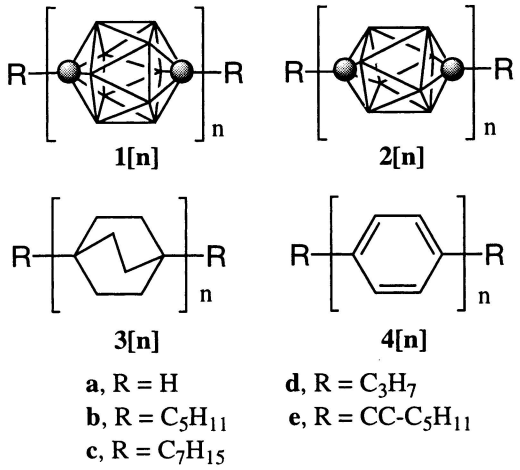

Figure 1. Derivatives of 1,12-dicarbadodecaborane (**1**[**1**]**a**), 1,10-dicarbadecaborane (**2**[**1**]**a**), bicyclo[2.2.2]octane (**3**[**1**]**a**) and benzene (**4**[**1**]**a**). In **1** and **2** each vertex corresponds to a BH fragment and the sphere represents a carbon atom.

*Author for correspondence;
e-mail: piotr@ctrvax.vanderbilt.edu

Liquid Crystals ISSN 0267-8292 print/ISSN 1366-5855 online © 2003 Taylor & Francis Ltd
http://www.tandf.co.uk/journals
DOI: 10.1080/0267829021000039669

effects on mesophase behaviour, we decided to examine series **1[1]b** and **2[1]b** in detail.

Here we describe mesogenic behaviour of two series of compounds in a nematic host and compare their virtual nematic-isotropic temperatures. The experimental results are discussed in the context of hard spherocylinders theory.

2. Results

2.1. *Synthesis*

The *p*-carborane derivatives were obtained by alkylation of *p*-carborane dimers, **1[2]a** and **2[2]a**, according to the method described before [4]. 1,4-Dipentylbenzene was prepared using the Kumada coupling [5] of $C_5H_{11}MgBr$ and 1,4-dichlorobenzene.

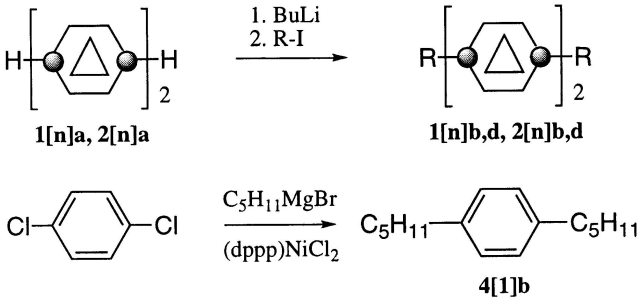

2.2. *Mesogenic properties*

Microscopic and thermal analyses of carborane dipentyl derivatives **1[2]b** and **2[2]b** showed that they exhibit enantiotropic nematic phases, while results for the hydrocarbons, **3[2]b** [6] and **4[2]b** [7], confirmed earlier reports of highly ordered smectic phases. Neither an enantiotropic nor a monotropic mesophase was observed for the dipropyl derivative **1[2]d**. For consistency of the results, we reproduced our earlier results for single ring compounds using a more sensitive DSC instrument. All results are collected in table 1.

Thermal analysis revealed that bicyclo[2.2.2]octane derivative **3[2]b** and two 12-vertex carborane derivatives, **1[2]b** and **1[2]d**, partially decompose upon heating above 220°C either in DSC or on a hot stage. The cooling curve for a sample of **3[2]b**, previously heated to 300°C, is featureless and microscopic observations show only an isotropic glassy substance. The transition temperatures and enthalpies for **3[2]b** were significantly lower after each heating cycle to 270°C indicating increasing amounts of impurities. Similar behaviour was observed for the **1[2]** derivatives.

Binary mixtures of **1b–4b** were studied in a weakly polar nematic host (figure 2) chosen in such a way to

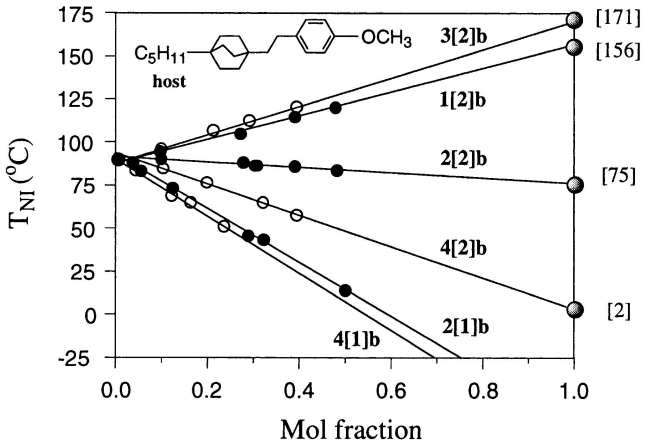

Figure 2. Nematic-isotropic transition temperatures T_{NI} as a function of concentration of dipentyl derivatives of carboranes (full circles) and carbocycles (open circles) in the host shown in the diagram. Best fit lines excluding $x = 0$: **1[2]b**, $y = 88 + x \cdot 68$ ($R^2 = 0.996$); **2[1]b**, $y = 93 - x \cdot 158$ ($R^2 = 0.999$); **2[2]b**, $y = 92 - x \cdot 17$ ($R^2 = 0.92$); **3[2]b**: $y = 88 + x \cdot 83$ ($R^2 = 0.996$); **4[1]b**: $y = 90 - x \cdot 166$ ($R^2 = 0.993$); **4[2]b**: $y = 95 - x \cdot 93$ ($R^2 = 0.999$). The circle on the vertical axis represents the N–I transition temperature for the pure host (89°C).

Table 1. Transition temperatures [°C] and enthalpies [kJ/mole].

Compound		Cr		S		N			I
1[1]b	$T/\Delta H$	•	16.2/19.1			•		[−18][a]	•
2[1]b	$T/\Delta H$	•	−5.8/13.5			•		[−65]	•
3[1]b	$T/\Delta H$	•	−13.7, −9.8/20.4[a]			•	(−24.5),	[−6][a]	•
4[1]b	$T/\Delta H$	•	−34.5/59.3 (49[b])			•		[−76]	•
1[2]b	$T/\Delta H$	•	154.2/21.7[c]			•	172.5/1.8,	[156]	•
2[2]b	$T/\Delta H$	•	84.0/16.6[d]			•	97.8/1.1,	[75]	•
3[2]b	$T/\Delta H$	•	41.0/16.5 (46[e])	•	243.9/12.5[f] (247[e])	•		[171]	•
4[2]b	$T/\Delta H$	•	13.1/6.7[g] (25.1[h])	•	50.2/13.1[g] (52.3[h])	•		[2]	•
1[2]d	$T/\Delta H$	•	240.0/26.6[f]						•

[a] Data from ref 3. [b] Petrov, A. D.; Nikishin, G. I.; Vorobev, V. D. *Bull Acad. Sci USSR, Div. Chem. Sci.* **1960**, 675. In this work, a sharp peak for crystallization of the liquid was observed at −54.3°C (peak max at −49.1°C). [c] Cr–Cr transitions observed on first heating at 74.6°C (7.0 kJ/mol) and 106.8°C (3.6 kJ/mol). [d] Cr–Cr transitions observed on first heating at 51.5°C (3.2 kJ/mol). [e] Ref 6. [f] Obtained at the heating rate of 10°C/min. Partial decomposition. [g] Multiple transitions. [h] Ref 7.

undergo the N–I transition ($T_{NI} = 89.1°C$) close to the middle of the range of expected clearing temperatures (−100°C to 250°C). Two-ring derivatives [**2**]**b** generally show ideal miscibility with the host. In contrast, mixtures containing more than 30 mol % of single-ring compounds, especially **4**[**1**]**b**, undergo phase separation upon cooling to a nematic phase. Some of the mixtures have a very strong tendency to form homotropic textures and are difficult to observe by optical microscopy. To assure consistency of the results, we reexamined phase diagrams for [**1**]**b** and used only the temperature of the first appearance of the nematic phase upon slow cooling (2°C/min) of the isotropic phase for the calculation of the virtual isotropic transition [T_{NI}]. The previous results for [**1**]**b** were confirmed except for **2**[**1**]**b**, for which the [T_{NI}] was found to be consistently higher than that reported previously [3].

Virtual nematic-isotropic transition temperatures, [T_{NI}], were obtained for **1**[**2**]**b**–**4**[**2**]**b**, **2**[**1**]**b** and **4**[**1**]**b** in a nematic host by extrapolation from at least four datapoints excluding that for the pure host (figure 2). The resulting [T_{NI}] and the previously obtained temperatures for **1**[**1**]**b** and **3**[**1**]**b** are shown in table 1. Inclusion of the datapoint for the pure host changes the extrapolated temperature up to +8°C for **4**[**2**]**b** and −4°C for **3**[**1**]**b**. The correlation factor R^2 is very high (⩾0.99) except for 10-vertex derivative **2**[**2**]**b**, for which non-linear behaviour is observed at low concentrations. Similar behaviour was observed before for the heptyl derivative **2**[**2**]**c** [2] and in both cases $R^2 \approx 0.92$.

The results show that virtual N–I transition temperatures [T_{NI}] for the smectic derivatives are significantly lower, by about 70°C for **3**[**2**]**b** and 50°C for **4**[**2**]**b**, than their corresponding enantiotropic S–I transition temperatures. The differences between the virtual and real N–I transitions temperatures are much smaller for **1**[**2**]**b** and **2**[**2**]**b** and are −17 and −24°C, respectively. The single ring bicyclo[2.2.2]octane derivative **3**[**1**]**b** is an exception and exhibits a positive difference of +18°C between the [T_{NI}] and (T_{NI}).

The extrapolated transition temperatures for **3**[**1**]**b** and **4**[**1**]**b** are significantly different from those obtained from a single concentration method in E7 host. The previously measured value for **3**[**1**]**b** ranges from −18°C for E7 host to −57°C for 5HE5, and the value for **4**[**1**]**b** was established to be −175°C in E7 [8]. These results show a significant host dependence for the extrapolated transition temperatures.

A correlation of [T_{NI}] for one-ring [**1**]**b** vs [T_{NI}] for two-ring compounds [**2**]**b** is shown in figure 3. The excellent correlation for three cylindrical compounds **1b–3b** indicates that addition of a homostructural ring to [**1**]**b** enhances the nematic phase stability [**2**]**b** proportionally to the performance of the single-ring compounds. Thus, the higher [T_{NI}] for one-ring compound, the higher [T_{NI}] for two-ring compound. Benzene derivatives **4b** deviate from this correlation, but nevertheless follow the general trend.

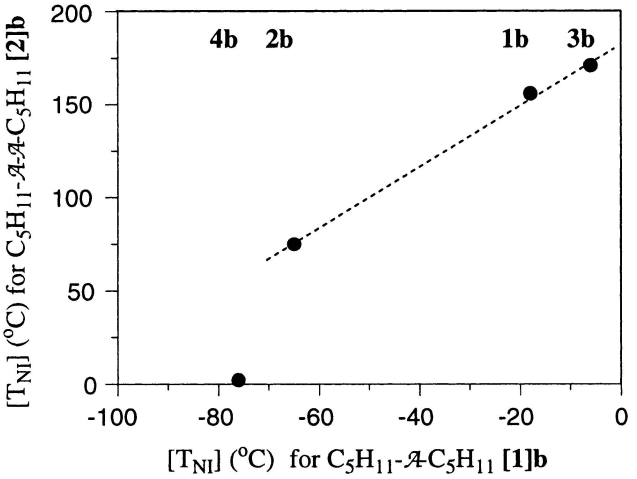

Figure 3. Virtual nematic-isotropic transition temperatures [T_{NI}] for single ring compounds vs [T_{NI}] for two ring compounds **1b–4b**. The best fit function for three point line (**1**, **2** and **3**): $T_{NI} = 1.65 \cdot [T_{NI}] + 183$; ($R^2 = 0.998$).

Figure 4 shows a correlation between clearing temperatures T_c for the pentyl derivatives [**2**]**b** and their heptyl analogs [**2**]**c**, and demonstrates an effect of extending of each alkyl chain by two CH_2 units on mesophase stability. The plot shows that the clearing temperature T_c for the three cylindrical heptyl derivatives **1**[**2**]**c**–**3**[**2**]**c** is lower, in amount proportional to the clearing temperature T_c, than the corresponding pentyl derivatives **1**[**2**]**b**–**3**[**2**]**b**. In contrast, the T_c for 4,4′-diheptylbiphenyl

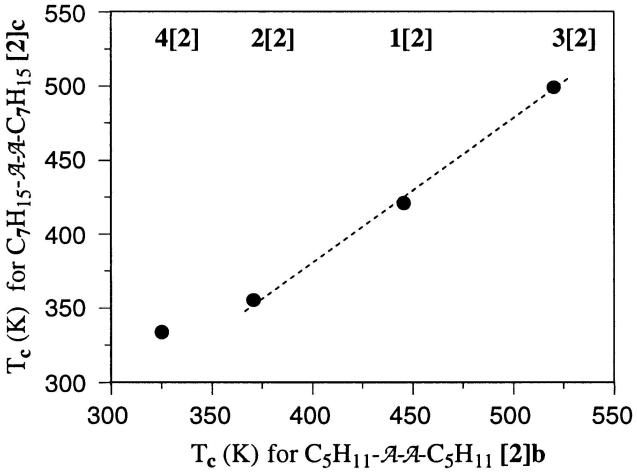

Figure 4. Clearing temperatures T_C for heptyl derivatives [**2**]**c** vs T_C for pentyl derivatives [**2**]**b**. The best fit function for three point line (**1**, **2** and **3**): T_C ([**2**]**c**) = 0.955 · T_C ([**2**]**b**); ($R^2 = 0.997$).

(**4**[**2**]**c**) is higher by 9°C than that for **4**[**2**]**b** [7]. This difference in trends is consistent with the generally observed changes in T_c for homologous series [9]. The decrease in T_c for high temperature mesogens (>70°C) has been ascribed to increased conformational mobility of longer alkyl chains and the entropic destabilization of the mesophase [10].

2.3. *Molecular modelling*

The change in molecular dimensions for dipentyl derivatives upon addition of a second ring to single-ring compounds was assessed using the MNDO method [11]. Thus geometry optimization was performed for all eight dipentyl derivatives at their conformational minima corresponding to the most extended molecular shapes. For biphenyl **4**[**2**]**b** the two benzene rings were constrained at 45 deg dihedral angle, to avoid an unrealistic orthogonal orientation of the rings in unconstrained calculations. After correcting for Van der Waals radii, each of the resulting molecules was fitted into a cylinder as shown for **2**[**1**]**b** in figure 5. The dimensions and volume of best cylinder, V_c, and the corresponding aspect ratio X for each compound are listed in table 2.

The calculations confirmed our previous computational and experimental findings on conformational properties of the rings. Thus, the relative orientation of the substituents in most preferred conformers of the *p*-carborane derivatives remains the same (antiperiplanar for **1**[**n**] and gauche for **2**[**n**]) for homologs with odd and even number of rings, while for the hydrocarbons the orientation of substituents alternates between gauche and antiperiplanar [3, 4]. This variation of conformational properties in the series of compounds affects the static aspect ratio X largely by influencing the length L. It presumably also affects the dynamic aspect ratio X_d since the most preferred antiperiplanar orientation cannot be achieved in all cases. Generally, the aspect ratio X is about 2.6–2.8 for single-ring compounds [**1**]**b** and about 3.1–3.3 for two ring mesogens [**2**]**b**. The difference corresponds to approximately 25% increase in X for **1** and **4**, 16% for **3** and only 10% for **2**. For comparison the aspect ratio for the host is 2.86.

A correlation between the calculated static aspect ratio X and the virtual clearing temperature [T_{NI}] is shown in figure 6. The vertical line separates the single-ring compounds [**1**]**b** from two-ring mesogens [**2**]**b** and

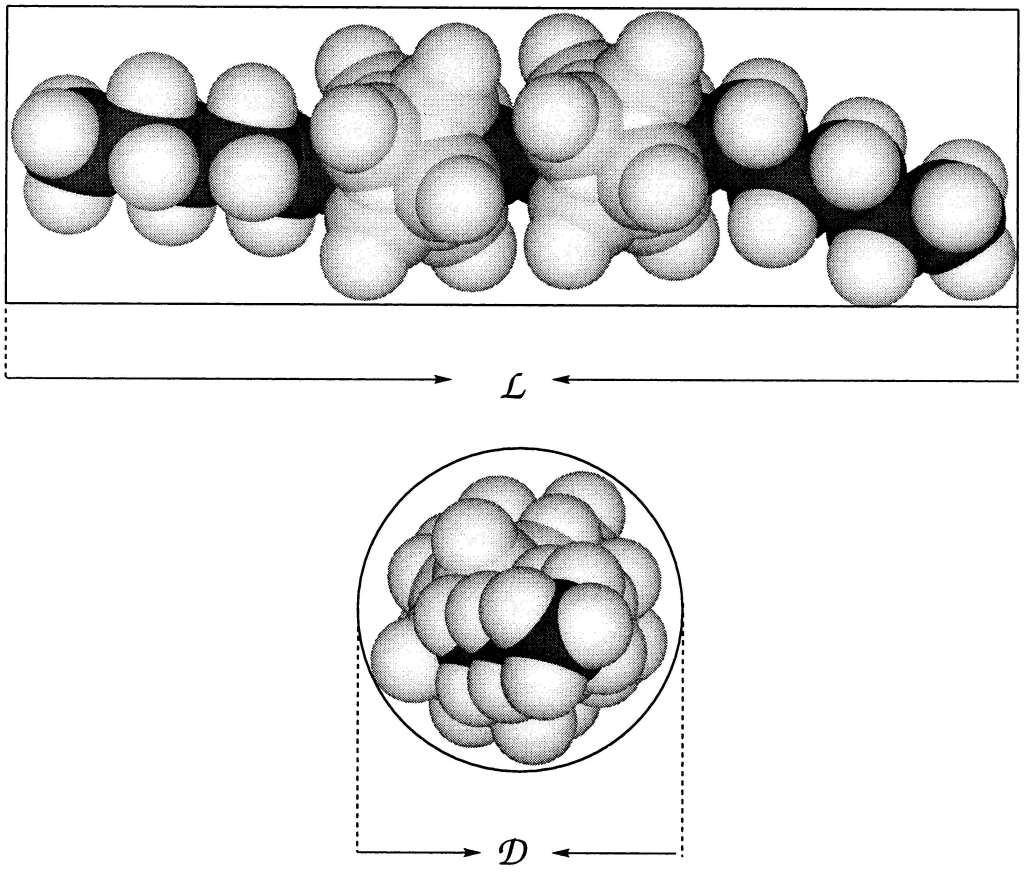

Figure 5. Best cylinder inscribed onto a molecule of **2**[**2**]**b**.

Table 2. Dimensions and volume of the best cylinders containing the Van der Waals molecular models V_C, aspect ratio X and filling fraction F.[a]

Compound	Length L [Å]	Width D [Å]	$X = L/D$	V_C[b] [Å^3]	V_B[c] [Å^3]	$F = V_B/V_C$
1[1]b	20.1	7.9	2.54	985	361	0.37
2[1]b	20.2	7.2	2.81	822	335	0.41
3[1]b	19.5	7.1	2.75	772	326	0.42
4[1]b	19.5	7.2	2.71	794	281	0.35
1[2]b	24.8	7.8	3.18	1185	520	0.44
2[2]b	24.6	7.9	3.11	1206	469	0.39
3[2]b	23.7	7.4	3.20	1019	443	0.43
4[2]b	23.3	6.9	3.38	871	360	0.41
host	20.9	7.3	2.86	875	377	0.43
1[2]e[d]	28.0	9.5	2.95	1985	567	0.29
2[2]e[d]	28.1	9.5	2.97	1992	519	0.26

[a] The molecular models were obtained by full geometry optimization for the conformation with most elongated shape using the MNDO method. [b] Volume of the best cylinder $V_C = 0.25 \cdot \pi \cdot L \cdot D^2$. [c] Van der Waals volume calculated in the Cerius2 suite of programs using keywords: VOLUME = TOTAL, GRID = FINE, PROBE RADIUS = 3.0. [d] Dimensions of the cylinder curved by alkyl groups free rotating around the ≡C–C bond.

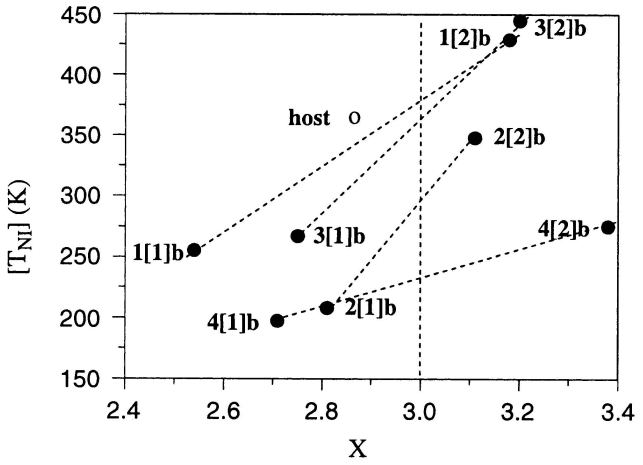

Figure 6. Virtual nematic-isotropic transition temperatures $[T_{NI}]$ vs aspect ratio X. Circle represents the host. Lines are guides for the eye.

is set at $X = 3$, which is comparable with the lower limit of the existence of a nematic phase for rod-like molecules. It is noticable, however, that **3[1]b** exhibits a monotropic nematic phase despite its relatively low aspect ratio ($X = 2.75$) [3] and the host ($X = 2.86$) is a broad temperature range nematic material. Among the two-ring mesogens, the three cylindrical derivatives **[2]b** show a steep increase in stability of the nematic phase with increasing X. Biphenyl **4[2]b** again does not follow this trend and the $[T_{NI}]$ is disproportionately low for its relatively high aspect ratio. In both, one- and two-ring series, 12-vertex carborane and bicyclo[2.2.2]octane derivatives, **1b** and **3b**, exhibit the highest transition temperatures $[T_{NI}]$.

Analysis of the data in figure 6 shows a large increase of the transition temperature $[T_{NI}]$ with a relatively small increase of X. The largest change is observed for the 10-vertex derivatives **2b** for which the ratio of $(\Delta[T_{NI}]/T_{NI})$ and $(\Delta X/X)$ is 6.2. The same ratio for benzene derivatives is 1.6 and is smallest in the series.

Figure 7 presents a correlation between a $[T_{NI}]$ and the filling fraction F defined as a ratio of the Van der Waals molecular volume, V_B [12], and the volume of the best cylinder, V_C. The graph shows that in contrast to other derivatives the filling fraction for BCO derivatives **3b** is little affected by addition of another BCO ring and both derivatives efficiently fill the best cylinder containing them. Addition of the second ring to 12-vertex and benzene derivatives, **1b** and **4b**, leads to a significant improvement in filling of the cylinder volume. Surprisingly, addition of a second 10-vertex ring to **2[1]b** causes a marked *decrease* in the filling fraction F in **2[2]b**.

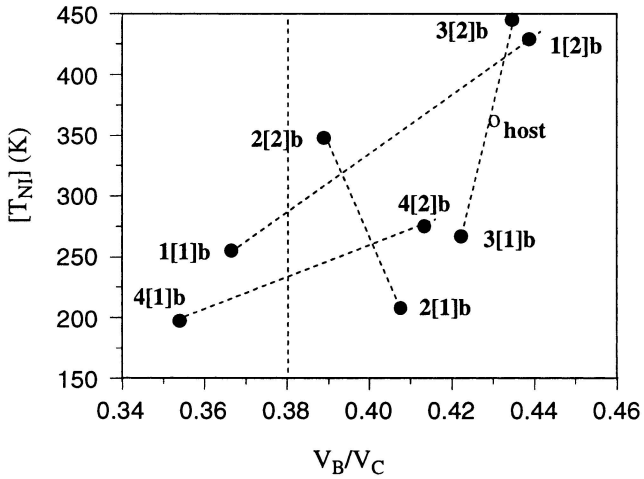

Figure 7. Virtual nematic-isotropic transition temperatures $[T_{NI}]$ vs filling fraction F. Circle represents the host. Lines are guides for the eye.

The calculated higher filling fraction F for 12-vertex than for the 10-vertex carborane is consistent with the experimental higher density of the solid [4] and liquid phases [13] for the former.

3. Discussion

Ideally, a comparison of the ability of molecular structural units to support mesogenic behaviour should be done for a series of simple, closely related pure materials exhibiting the same, preferably nematic, phase. Unfortunately, direct comparison of effectiveness of rings **1–4** in stabilization of a mesogenic phase is complicated by the diverse behaviour of the two series of dipentyl derivative **1b–4b**. Thus, single-ring compounds are non-mesogenic in the pure state except for the bicyclo[2.2.2]-octane derivative **3**[**1**]**b** which exhibits a monotropic nematic phase [3]. In contrast, the two ring analog **3**[**2**]**b** is a highly ordered smectic, while the carborane derivatives, **1**[**2**]**b** and **2**[**2**]**b**, form nematic phases. In such a situation, a comparison of virtual nematic-isotropic transition temperatures obtained for all compounds in the same host appears to be a reasonable choice.

The choice of matrix is critical since the virtual temperature [T_{NI}] shows a significant matrix dependence [8]. For instance, the previously measured value for **3**[**1**]**b** ranges from -18°C in E7 host to -57°C in 5HE5 (an aromatic ester) [8], while our value is -6°C. Also the [T_{NI}] for the two-ring homolog **3**[**1**]**b** is lower by 18°C than that extrapolated from 10 mol % solution in ZLI-4792 [14]. The matrix effect on [T_{NI}] is most dramatic for **4**[**1**]**b**, for which the difference between our result in a weakly polar host and that obtained from the polar E7 host [8] is about $+100^{\circ}$C. In contrast to our results, however, the previously reported [T_{NI}] values were extrapolated from a single concentration, and some hosts, e.g. E7 [8], show significant non-linear behaviour in some binary mixtures.

As imperfect this comparison of [T_{NI}] is, it clearly gives a consistent order of ring effectiveness in mesophase stabilization. Thus the order of [T_{NI}] is as follows: BCO > 12-vertex > 10-vertex > benzene (**3** > **1** > **2** > **4**) and is identical to the order of clearing temperatures T_c for pure two-ring compounds. This suggests that specific interactions between the solute and the host are either reasonably low or similar for all compounds in the considered series, and we can assume that they behave as ideal solutions around the N–I transition.

It is apparent from figures 3, 4, and 6 that three spherocylindrical molecules **1b–3b** show similar coherent mesogenic behaviour, while benzene derivatives **4b** stands out from the series. Extension of molecular length gives a large increase in mesophase stability for the three molecular systems **1b–3b**, but has a relatively small effect for the benzene derivatives **4b**.

Some insight into the factors contributing to the stability of the nematic phase for each series of compounds **1b–4b** can be obtained through an analysis of these results in terms of the Generalized Van der Waals (GVDW) theory of the nematic state [15]. For the purpose of this qualitative comparison, it can be assumed that the density of the nematic phase and the order parameter are approximately the same for all compounds at low concentrations and not much different from those of the pure host. Therefore, it can be assumed that the packing fraction for the compounds considered here is proportional to a filling fraction $F = V_B/V_C$.

It follows from the GVDW theory that the transition temperature T_{NI} is approximately proportional to the static aspect ratio X. Since the packing fraction $P = V_B/V$ (where V is a single molecule volume in condensed phase) is also almost a linear function of X, then T_{NI} should depend approximately linearly on the packing fraction P. In these correlations, the slope is largely dependent on the isotropic pseudopotentials L_0 and the intercept is related mainly to the anisotropic pseudopotential L_2 [9].

The aspect ratio X and packing fraction (or filling fraction) are considered to be important indicators for nematogenic behaviour of compounds. Figures 6 and 7 show that compounds with static aspect ratio $X \geqslant 2.8$ and filling fraction $F \geqslant 0.38$ exhibit mesogenic behaviour. BCO derivatives exhibit an exceptional tendency for the formation of the nematic phase despite a relatively low aspect ratio (2.75 for **3**[**1**]**b** or 2.86 for the host). This can be ascribed to high filling fractions for these derivatives ($F \geqslant 0.4$) and relatively high conformational rigidity of the alkyl-BCO bond (table 3). In contrast, **2**[**1**]**b** is conformationally flexible and despite a relatively

Table 3. Calculated (HF/6-31G*) enthalpy and free energy differences between conformational extremes in 1-ethyl derivatives of the parent rings **1**[**1**]**a**–**4**[**1**]**a**.[a]

	ΔH	ΔG_{298}
1-Et-*p*-$C_2B_{10}H_{11}$[b]	0.12	1.32
1-Et-*p*-$C_2B_8H_9$[b]	0.45	1.62
1-Et-C_8H_{13}[c]	4.33	3.89
1-Et-C_6H_5[d]	0.88	2.54

[a] Energy in kcal/mol. Data taken from ref. 4. [b] Difference between the staggered and eclipsed conformations. [c] Difference between the eclipsed and staggered conformations. [d] Difference between the orthogonal orientation of the ethyl group and the TS in which the Et group is about 11 deg off the benzene plane. The local planar (C_s) conformational minimum is higher in energy than the global minimum: $\Delta H = +1.47$ kcal/mol; $\Delta G_{298} = +0.80$. These results are in agreement with experimental data: Schafrenberg, P., *J. Chem. Phys.*, **1982**, 77, 4791–4793, and references cited therein.

high filling fraction ($F = 0.41$), it does not exhibit mesogenic behaviour.

The significance of the aspect ratio X, the filling fraction F, and molecular rigidity is evident from the surprisingly poor mesogenic behaviour of two acetylene derivatives **1**[**2**]**e** and **2**[**2**]**e**. Typically, X is calculated as a static aspect ratio for a molecule in conformational minima corresponding to the most elongated molecular shape. Acetylene derivatives **1**[**2**]**e** and **2**[**2**]**e**, however, have no conformational minima and the alkyl chains rotate freely around the Alk–C≡ bond. In this case the aspect ratio is calculated as a ratio of a the length to the diameter of a cylinder defined by the cone of the freely rotating alkyl chain. Thus replacement of a $-CH_2CH_2-$ fragment in each chain of **1**[**2**]**c** and **2**[**2**]**c** by –C≡C– in **1**[**2**]**e** and **2**[**2**]**e** activates the free rotation and results in a low aspect ratio ($X = 2.95$, table 2), a low filling fraction ($F < 0.3$, table 2), and a dramatic depression of the clearing point by >150 K. On the other hand, stiffening of the molecule and increasing the filling fraction F by perfluorination of the central ethylene linker in a 1,2-dicyclohexylethane mesogen significantly increases the clearing temperatures (by up to 70 K) [16].

The commonly used static aspect ratio X in the GVDW theory instead of the more appropriate dynamic aspect ratio X_d represent a reasonable compromise dictated by practical reasons. Undoubtedly, the dynamic aspect ratio X_d, obtained for a weighted average of all conformations present in condense phase at given temperature, describes correctly the molecular shape of a molecule in the nematic phase [17]. As such an extensive conformational analysis is not trivial albeit possible [17–21], it is assumed that aspect ratio X obtained for a single conformer in its most elongated molecular shape and corresponding global conformational energy minimum reasonably approximates the dynamic X_d. This approach may work reasonably well for many molecuar systems, but for some the approximation may not properly reflect the dynamic behaviour of the molecule. Thus the use of X excludes, of course, gauche conformations of the alkyl chain and other higher energy conformations that would adjust the molecular shape to fit the molecular cavity in the nematic continuum better. In extreme cases, such as acetylenes **1**[**2**]**e** and **2**[**2**]**e**, there are no conformational minima and it is reasonable to assume the average molecular dimensions for a freely rotating molecular subunits.

Results presented in figure 6 show that the increase in T_{NI} relative to ΔX (the slope) for the three cylindrical molecules **1–3** is similar, which suggests similar isotropic pseudopotentials L_0 for these three ring systems. The relatively small $\Delta T_{NI}/\Delta X$ for **4b** suggests a low isotropic pseudopotential L_0.

These observed differences in $\Delta T_{NI}/\Delta X$ can be attributed to the packing fraction P in the nematic phase or to the filling fraction F. As the data in table 2 shows, the value of F varies significantly for all considered molecules and hence the best cylinders have different 'density'. It can be expected that 'lighter' or less 'dense' cylinders will interact less strongly (lower pseudopotential) than the 'heavier' ones. This is largely due to fewer electrons, lower overall electronic polarizability and generally larger intermolecular distances and hence much weaker dispersive attractive forces, which are key components of the isotropic pseudopotential L_0. Normalization of the aspect ratio X with respect to the filling fraction F should give similar proportional increase in nematic phase stability (lines with similar slopes) indicating similar influence of the isotropic potential L_0 on T_{NI} in all four series of compounds. Indeed, figure 8 shows that three derivatives **2b–4b** have similar $\Delta T_{NI}/\Delta(X/F)$, while the slope for 12-vertex derivatives is markedly higher. The intercept of the lines connecting [**1**] and [**2**], related to the magnitude of the anisotropic pseudopotential L_2, increases from Ph to BCO.

The higher slope for **1b** than for other compounds suggests stronger intermolecular interactions of the 12-vertex cluster with the matrix than would result from dispersive interactions alone. A plausible candidate causing the additional stabilization effect is the electronic polarizability and quadrupole moment which are the largest for the 12-vertex cage, as evident from table 4.

All results and analyses show strong stabilizing effects of 12-vertex and BCO on the nematic phase. Considering the electronic and conformational properties of the rings

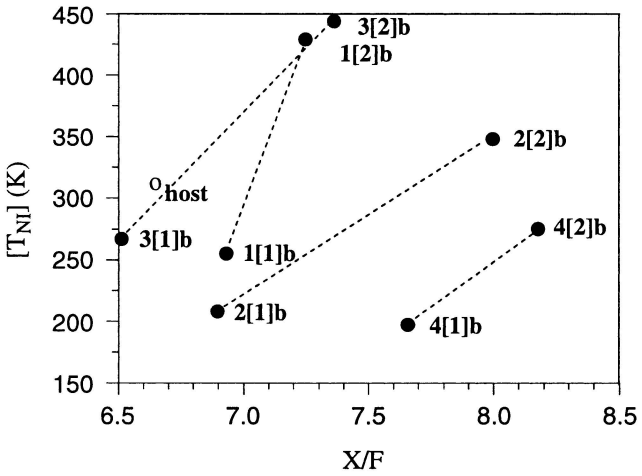

Figure 8. Virtual nematic-isotropic transition temperatures [T_{NI}] vs aspect ratio X normalized with respect to filling fraction F. Circle represents the host. Lines are guides for the eye.

Table 4. Electronic polarizability and quadrupolar moments for parent rings.[a]

	Polarizability [Å^3]			Quadrupole moments [$D \cdot$ Å]		
	$\alpha_{\parallel}$	$\Delta\alpha$	α_{avrg}	$Q_{\parallel}$	ΔQ	Q_{avrg}
1[**1**]**a**	108	−7	113	−71	11	−78
2[**1**]**b**	96	1	95	−58	10	−64
3[**1**]**a**	74	0	74	−52	0	−52
4[**1**]**a**	68	47	52	−31	4	−34

[a] Obtained at the HF/6-31G* level of theory and taken from ref. 4.

(tables 3 and 4) the stabilizing effect of BCO can be ascribed to conformational rigidity of its alkyl derivatives (high barrier to internal rotation) and efficient packing (high filling fraction). In contrast, the 12-vertex carborane has poor compatibility with alkyl chains (low filling fraction) and its derivatives are conformationally flexible (low barrier to internal rotation). The cluster has, however, the largest electronic polarizability and quadrupole moment among the rings that drive the molecular pseudopotentials. This results in strong intermolecular interactions and may give rise to specific intermolecular interactions in the condensed phase. The 10-vertex carborane has less favorable electronic properties than the 12-vertex analog, which is reflected in the significantly lower stabilization of the nematic phase. The least favorable factors, both electronic and steric, are found for benzene.

The above conclusions are consistent with other results obtained for boron cluster derivatives. For instance, our studies showed that fluid and solid phases of **1**[**2**]**c** are more dense than those of the 10-vertex analog [4, 13]. The 10-vertex cluster derivatives generally exhibit difficulties in efficient packing in the solid phase, evident from single crystal X-ray analysis for **2**[**2**]**c** and **2**[**2**]**e**, which are presumably related to peculiar symmetry properties of the cluster and the distribution of conformational minima of the substituents.

The 12-vertex cluster has high electronic polarizability reflected in high refraction of pure mesogens [22], nematic mixtures [23, 24], and non-mesogenic compounds [25, 26]. Some of 12-vertex cluster derivatives appear to exhibit specific intermolecular interactions in the condensed phase which stabilize the liquid crystalline phase. For instance, an anomalous stabilization of a S_E phase was observed in a binary mixture with a terphenyl host [27]. In another case, changing an ester group to an ether causes a significant increase, by about $+70^{\circ}$C, of the T_{NI} [28]. In both cases the effect can be attributed to the presence of the alkoxyphenyl fragment and its specific intermolecular interactions with the 12-vertex carborane cluster. These interaction may be responsible for the higher isotropic pseudopotential for **1b** (figure 7) since the host contains a methoxyphenyl group.

The consequence of the high molecular potential and high energy of interaction with the nematic continuum is the viscosity or the resistance to changes in relative molecular orientations. Thus, the relatively high viscosity of BCO derivatives [29] can be related to the low conformational flexibility of the alkyl-BCO bond and the high filling fraction F. In contrast, the high viscosity of 12-vertex derivatives [23, 24] can be ascribed to the high molecular polarity and the resulting 'stickiness' of the cage.

4. Conclusions

Analysis of results for the four pairs of dipentyl derivatives shows that the aspect ratio, filling fraction (packing fraction), conformational mobility and polarity are key factors affecting the stability of a nematic phase. The highly nematogenic properties of the BCO derivatives can be ascribed to the low conformational mobility of the substituents on the bicyclo[2.2.2]octane ring and the high filling fraction. In contrast, the high stability of 12-vertex carborane compounds is presumably solely due to a large polarizability and quadrupole moment of the cage. Both carboranes have relatively low barrier to internal rotation around the alkyl-carborane bond (high conformational mobility) and, due to the size disparity between the substituents and the cage, a low filling factor. The lower aptitude of 10-vertex carborane in stabilization of the nematic phase is presumably related to its unfavorable symmetry properties, which affect the distribution of conformational minima and consequently static aspect ratio X. The relatively poor performance of Ph in stabilization of a nematic phase is due to the low filling fraction.

Generally, symmetry and conformational properties play an important role in the stability of a nematic phase by defining the conformational mobility, aspect ratio X and dimension for the best cylinder V_c, and hence the filling fraction F. Besides the conformational properties, filling fraction F is also critically dependent on the size compatibility of the molecular constituents. The diameter of the BCO ring is similar to the cross section of an alkyl chain, which leads to the efficient filling of a spherocyllindrical space. Similarly high filling fractions could be obtained for 12-vertex carborane derivatives by using fluorinated alkyl chains.

5. Experimental Section

The phase transition points of the compounds and their mixtures were determined using a PZO 'Biolar' polarized microscope equipped with a HCS250 Instec hot stage. Thermal analysis was obtained using a TA

Instruments 2920 DSC. Transition temperatures (onset) and enthalpies were obtained using small samples (2–3 mg) and a heating rate of 2°C min^{-1}. The phase diagrams were determined by the single concentration method. For mixtures the transition temperatures were taken as the upper limit of the biphasic region as observed by optical microscopy. Homogenous mixtures were prepared by evaporation of the CH_2Cl_2 solutions from which the solvent was removed by heating the samples at 80°C for 2 hr. Mixtures with two-ring mesogens were additionally dried under vacuum (~3 Torr) at ambient temperature for several hours. Before each experiment the mixtures were conditioned at a nematic phase (>90°C) for 1 hr. NMR spectra were obtained on a Bruker 300 MHz instrument in $CDCl_3$ and referenced to $CHCl_3$ (^{1}H NMR) and $CDCl_3$ (^{13}C NMR) unless stated otherwise. Mass spectrometry was performed using a Hewlett-Packard 5890 instrument (GCMS). Elemental analysis was provided by Atlantic Microlab, Norcross, Georgia.

*1,1′-Bis[12-pentyl-1,12-dicarba-closo-dodecaborane] (**1[2]b**).* The crude compound prepared according to a general procedure [4] was purified by gradient sublimation at 145°C/0.1 Torr, double recrystallization from heptane, and another gradient sublimation: ^{1}H NMR δ 0.80 (t, $J = 7.2$ Hz, 6H), 1.00–1.07 (m, 8H), 1.12–1.24 (m, 4H), 1.46–1.55 (m, 4H); EIMS *m/e*: 401–390 (max at 397, 100%, M-Et). Anal. Calcd for $C_{14}H_{42}B_{20}$: C 39.41, H 9.92. Found C 39.54 H, 10.06%.

*1,1′-Bis[12-propyl-1,12-dicarba-closo-dodecaborane] (**1[2]d**).* The crude compound prepared according to a general procedure [4] was fractionally sublimed and recrystallized twice from heptane: ^{1}H NMR δ 0.70 (t, $J = 7.3$ Hz, 6H), 1.01–1.15 (m, 4H), 1.46–1.52 (m, 4H); EIMS, *m/e*: 374–364 (max at 370, 100%, M^+). Anal. calcd for $C_{10}H_{34}B_{20}$: C 32.41, H 9.25. Found C 32.56; H, 9.37%.

*1,1′-Bis[10-pentyl-1,10-dicarba-closo-decaborane] (**2[2]b**).* The crude material prepared according to a general procedure [4] was vacuum distilled, twice recrystallized from EtOH and fractionally sublimed: ^{1}H NMR δ 0.98 (t, $J = 7.1$ Hz, 6H), 1.41–1.57 (m, 8H), 1.92–2.01 (m, 4H), 3.22 (t, $J = 8.3$, 4H); ^{13}C NMR δ 14.10, 22.72, 23.37, 30.59, 31.46, 32.94, 41.86; EIMS *m/e*: 382–373 (max at 380, 43%, M^+), 352–345 (max at 350, 100%). Anal. calcd for $C_{14}H_{38}B_{16}$: C, 44.32; H, 10.09; found: C, 44.93, H 10.23.

*1,1′-Bis[4-pentylbicyclo[2.2.2]octane] (**3[2]b**)* [6]. The compound was used as received: ^{1}H NMR δ 0.86 (t, $J = 7.1$ Hz, 6H), 0.96–1.03 (m, 4H), 1.10–1.34 (m, 36H); ^{13}C NMR δ 14.09, 22.71, 23.45, 25.43, 29.88, 31.28, 32.91, 34.71, 41.69; EIMS *m/e*: 358 (45%, M^+), 329 (79%), 287 (100%).

*1,4-Dipentylbenzene (**4[1]b**)* [30]. 1,4-Dichlorobenzene (1.51 g, 10 mmol) in dry ether (20 mL) was reacted with pentylmagnesium bromide (2.0 M, 13 mL) in the presence of (dppp)$NiCl_2$ (0.10 g) according to the general Kumada procedure [5]. Pure product was isolated by fractional distillation (bp. 167°C/19 Torr, lit. [30] 170–175°C/25 Torr): ^{1}H NMR δ 0.89 (t, $J = 6.9$ Hz, 6H), 1.26–1.36 (m, 8H), 1.54–1.65 (m, 4H), 2.56 (t, $J = 7.8$, 4H), 7.08 (s, 4H); ^{13}C NMR δ 14.03, 22.57, 31.28, 31.59, 35.55, 128.22, 140.07; EIMS *m/e*: 218 (26%, M^+), 161 (100%).

*4,4′-Dipentyl-1,1′-biphenyl (**4[2]b**)* [7]. The biphenyl was recrystallized twice from EtOH before analysis: ^{1}H NMR δ 0.90 (t, $J = 6.6$ Hz, 6H), 1.28–1.38 (m, 8H), 1.60–1.70 (m, 4H), 2.63 (t, $J = 7.6$, 4H), 7.23 (d, $J = 8.1$, 4H), 7.49 (d, $J = 8.1$, 4H); ^{13}C NMR δ 14.05, 22.57, 31.20, 31.57, 35.57, 126.80, 128.74, 138.48, 141.75; EIMS *m/e*: 294 (39%, M^+), 237 (100%), 180 (65%). Anal. calcd for $C_{22}H_{30}$: C, 89.73, H 10.27; found: C, 89.96; H, 10.41.

This project has been supported in part by the NSF CAREER (DMR-9703002) and by Polish NATO Fellowship Foundation (WP). We are grateful to Dr. Volkmar Reiffenrath, of E. Merck for his generous gift of **3[2]b**, and to Professor Roman Dabrowski for the gift of the nematic host and dipentylbiphenyl (**4[2]b**).

References

§The NATO fellow on leave from Military University of Technology, Warsaw, Poland.

[1] Kaszynski, P., and Douglass, A. G., 1999, *J. Organomet. Chem.*, **581,** 28.

[2] Czuprynski, K., and Kaszynski, P., 1999, *Liq. Cryst.*, **26,** 775.

[3] Douglass, A. G., Both, B., and Kaszynski, P., 1999, *J. Mater. Chem.*, **9,** 683.

[4] Kaszynski, P., Pakhomov, S., Tesh, K. F., and Young, V. G. Jr., 2001, *Inorg. Chem.*, **40,** 6622.

[5] Tamao, K., Sumitani, K., Kiso, Y., Zembayashi, M., Fujioka, A., Kodama, S., Nakajima, I., Minato, A., and Kumada, M., 1976, *Bull. Chem. Soc. Jpn.*, **49,** 1958.

[6] Reiffenrath, V., and Schneider, F., 1981, *Z. Naturforsch.*, **36a,** 1006.

[7] Czuprynski, K., Przedmojski, J., and Baran, J. W., 1995, *Mol. Cryst. Liq. Cryst.*, **260,** 435.

[8] Abdullah, H. M., Gray, G. W., and Toyne, K. J., 1985, *Mol. Cryst. Liq. Cryst.*, **124,** 105.

[9] Demus, D., and Hauser, A., 1990, In *Selected Topics In Liquid Crystal Research*, edited by H. D. Koswig (Berlin: Akademie–Verlag), pp 19–44, and references therein.

[10] Toriumi, H., and Samulski, E. T., 1983, *Mol. Cryst. Liq. Cryst.*, **101,** 163.

[11] Dewar, M. J. S., and McKee, M. L., 1980, *Inorg. Chem.*, **19,** 2662.

[12] V_B was calculated for MNDO-optimized molecular models in a Cerius2 suite of programs using keywords volume = TOTAL, probe radius = 3.0 and grid = FINE.

[13] Piecek, W., Perkowski, P., Kaszynski, P., in preparation.
[14] Reiffenrath, V., personal communication.
[15] Cotter, M. A., 1977, *J. Chem. Phys*., **67,** 4268.
[16] Kirsch, P., Bremer, M., Huber, F., Lannert, H., Ruhl, A., Lieb, M., and Wallmichrath, T., 2001, *J. Am. Chem. Soc*., **123,** 5414.
[17] Emsley, J. W., Luckhurst, G. R., and Stockley, C. P., 1982, *Proc. R. Soc. London*, **A381,** 117.
[18] Garcia, E., Glaser, M. A., Clark, N. A., and Walba, D. M., 1999, *J. Mol. Struct. (THEOCHEM)*, **464,** 39.
[19] Glaser, M. A., 2000, *NATO Sci. Ser., Ser. C*., **545,** 263.
[20] Wilson, M. R., 1999, in *Structure and Bonding*, edited by D. M. P. Mingos (New York: Springer), **94,** pp 41–64.
[21] Crain, J., and Komolkin, A. V., 1999, *Adv. Chem. Phys*., **109,** 39.
[22] Douglass, A. G., Czuprynski, K., Mierzwa, M., and Kaszynski, P., 1998, *J. Mater. Chem*., **8,** 2391.
[23] Poetsch, E., personal communication.
[24] Chisso Petrochemical Corporation, personal communication.
[25] Fein, M. M., Grafstein, D., Paustian, J. E., Bobinski, J., Lichstein, B. M., Mayes, N., Schwartz, N. N., and Cohen, M. S., 1963, *Inorg. Chem*., **2,** 1115.
[26] Orlov, V. M., Pustobaev, V. N., Poroshina, T. Y., Ol'shevskaya, V. A., Zakharkin, L. I., and Gal'chenko, G. L., 1989, *Dokl. Akad. Nauk SSSR, Phys. Chem. (Engl. Transl.)*, **309,** 968.
[27] Douglass, A. G., Czuprynski, K., Mierzwa, M., and Kaszynski, P., 1998, *Chem. Mater*., **10,** 2399.
[28] Kulikiewicz, K. K., Januszko, A., Pakhomov, S., Kaszynski, P., and Douglass, A. G., in preparation.
[29] Carr, N., Gray, G. W., and Kelly, S. M., 1985, *Mol. Cryst. Liq. Cryst*., **130,** 265.
[30] Cram, D. J., and Daeniker, H. U., 1954, *J. Am. Chem. Soc*., **76,** 2743.